Parasitol Res (2017) 116:1937–1945
DOI 10.1007/s00436-017-5472-4

ORIGINAL PAPER

Study on the tolerance and adaptation of rats to *Angiostrongylus cantonensis* infection

Liu Ji[1,2,3] · Xu Yiyue[4,5] · He Xujin[6] · Zheng Minghui[7] · Zhang Mengying[1,2,3] · Hu Yue[1,2,3] · Wu Yanqi[1,2,3] · Song Langui[1,2,3] · Zeng Xin[1,2,3] · Lin Datao[1,2,3] · Wan Shuo[1,2,3] · Zheng Huanqin[1,2,3] · Wu Zhongdao[1,2,3] · Lv Zhiyue[1,2,3]

Received: 26 March 2017 / Accepted: 2 May 2017 / Published online: 11 May 2017

Abstract *Angiostrongylus cantonensis* (*A. cantonensis*) is the most common infectious agent causing eosinophilic meningitis. As an important food-borne parasitic disease, angiostrongyliasis cantonensis is an emerging infectious disease which brings severe harm to central nerve system of human. Rat, one of the few permissive hosts of *A. cantonensis* known to date, plays an indispensable role in the worm's life cycle. However, the tolerance and adaptation of rat to *A. cantonensis* infection is rarely understood. In this study, we infected rats with different numbers the third stage larvae (L3) of *A. cantonensis* and explored their tolerance through analysis on survival curve, neurological function score, and detection of pathological damages in organs including the brain, lung, and heart of the animals. Results indicated that rats' survival condition worsens, and body weight dropped more significantly as more worms were used for infection. Death appeared in groups infected with 80 and more *A. cantonesnsis* per rat. Morris water maze revealed that the neurological function of rats damaged gradually with increasing infection number of *A. cantonensis* larvae. When the number of infected parasite exceeded 240 per animal, rats showed significant neurological impairments. Collection of *A. cantonensis* from rat lung after 35 days of infection implied an upper limit for worm entry, and the average length of worm was inversely proportional to the infection amount, while the ratio between female and male worms was positively related to the infection number. The degree of pulmonary and cardiac inflammation was proportional to the infection number of *A. cantonensis*. Meanwhile, there existed considerable amount of adult worms in rat's right atrium and right ventricle, leading to a right heart myocardial inflammation. The present study firstly reports the tolerance and adaptation of rat, a permissive host of *A. cantonensis* to its infection, which will not only provide accurate technical parameters for maintaining *A. cantonensis* life cycle under laboratory conditions but also help unveil the underlying mechanism of the distinct pathological outcomes in the permissive and non-permissive hosts with *A. cantonensis* infection.

Keywords *Angiostrongylus cantonensis* · Rat · Tolerance · Adaptation

Liu Ji, Xu Yiyue, and He Xujin are the joint first authors.

✉ Lv Zhiyue
lvzhiyue@mail.sysu.edu.cn

[1] Zhongshan School of Medicine, Sun Yat-sen University, 74 2nd Zhongshan Road, Guangzhou 510080, China

[2] Key Laboratory of Tropical Disease Control, Ministry of Education, Sun Yat-sen University, Guangzhou 510080, China

[3] Provincial Engineering Technology Research Center for Biological Vector Control, Guangzhou 510080, China

[4] School of Life Sciences, The Chinese University of Hong Kong, Hong Kong, SAR, China

[5] State Key Laboratory of Agrobiotechnology, The Chinese University of Hong Kong, Hong Kong, SAR, China

[6] The Affiliated High School of South China Normal University, Guangzhou 510630, China

[7] Department of Clinical Laboratory, Sun Yat-sen Memorial Hospital of Sun Yat-sen University, Guangzhou 510120, China

Introduction

The rat lungworm *Angiostrongylus cantonensis* (*A. cantonensis*, Nematoda: Metastrongylidae) was firstly discovered in the pulmonary vessels of rat and named and classified in 1935 (Chen 1935). The hosts of *A. cantonensis* can be classified as permissive and non-permissive hosts based on

whether the worms could migrate to and mature in the lung of the hosts. In permissive hosts, such as rats, *A. cantonensis* can migrate from the brains into the lung where they sexually maturate, with slight eosinophilic inflammation and nerve damages. By contrast, in mice or human (the non-permissive host of *A. cantonensis*), the worms fail to migrate to the lung for sexual maturation but develop into the fifth stage larvae in the brain, where they die and cause severe meningitis or meningoencephalitis characterized by increasing eosinophils infiltration (Wang et al. 2012; Li et al. 2014a, b). The first case of human infected with *A. cantonensis* was reported in Taiwan in 1945, and new infections in human raised in mainland China, Thailand, Brazil, and the USA afterwards. As a public health issue, angiostrongyliasis cantonensis gains increasing attention recently (New et al. 1995; Tsai et al. 2004; Lv et al. 2009; McBride et al. 2017).

In the recent decades, a plethora of researches have been explored to develop integrated strategies for the prevention and control of angiostrongyliasis cantonensis (Eamsobhana 2014). Since both mouse and human are the non-permissive hosts of *A. cantonensis*, mouse has become the most widely used animal model in studies on invasion, migration and survival of the parasite, and coevolution between host and parasite (Liu et al. 2017; Feng et al. 2015). On the other hand, it is obvious that study on the interaction between *A. cantonensis* and its permissive host, rat, and the tolerance of rat to its infection will offer additional valuable clues for clarifying the serious pathological injury caused by *A. cantonensis* in non-permissive hosts.

In the present study, we infected rats with a series of numbers of the third stage larvae (L3) of *A. cantonensis* by intragastric administration followed by evaluation on the survival condition, neurological functions, immunopathological damage to the brain, lung, and heart of the infected animals, and counting the worms and calculation of the ratio between harvested adult female to male worms in order to gain a better insight on the tolerance of rat to *A. cantonensis* infection.

Method and materials

Animals

Sixty Sprague-Dawley (SD) rats (6–8 weeks old) were purchased from the Experimental Animal Centre of Sun Yat-sen University (SYSU) in this study. The experimental protocols were approved by the Institutional Animal Care and Use Committee of SYSU. All of the rats were housed in a specific pathogen-free environment, and the procedures done were in accordance with the regulations of the Guide for the Care and Use of Experimental Animals of the National Institutes of Health. Rats were randomly divided into 12 groups (5 rats per group), and they were orally infected with L3 of *A. cantonensis*. The 12 groups were named according to the number of worms used per rat for infection: group G0 (0 worm per rat), group G5 (5 worms per rat), group G10 (10 worms), group G20 (20 worms per rat), group G40 (40 worms per rat), group G80 (80 worms per rat), group G120 (120 worms per rat), group G160 (160 worms per rat), group G200 (200 worms per rat), group G240 (240 worms per rat), group G280 (280 worms per rat), and group G320 (320 worms per rat).

Parasites preparation

All of the L3 of *A. cantonensis* for infection in this study were obtained from *Biomphalaria glabrata* of 21 days post infection with the first stage larvae (L1) of the parasite. The snails were homogenized and digested in a pepsin-HCl solution (pH 2.0, 500 IU pepsin/g tissue) at 37 °C with incubator for 2 h. Then, the infective L3 were washed in phosphate-buffered saline (PBS) and counted under an anatomical microscope for infection on animals.

Rat survival status monitor

The body weight of each rat was measured and recorded on the daily base. The body weight of the rat in each group were statistically analyzed at 30 days post infection by comparing the change with their original weight. Meanwhile, the survival status of each group was observed. The changes of symptoms and death in each group were recorded every day for plotting survival curves.

Neurological function evaluation

After infection for 21 days, the neurological function of rats were assessed with the Morris water maze (MWM) by the experimental apparatus (RWD Life Science, Shenzhen, China) (Zhang et al. 2015). Memory training was performed for five consecutive days, and the rats were trained in four quadrants, then followed by a spatial probe task on the 7th day. The rat had to swim until it climbed onto the escape platform. Animals that failed to find the platform within 120 s were gently guided to the platform. At the end of each trial, animals were allowed to stay on the platform for 10 s. The probe task was done in the third quadrant (Jiang et al. 2015). The swim escape latency, average swim speed, time spent in the target quadrant, and number of times the rats crossed the previous location of the platform were recorded by a video tracking system (Taimeng Tech, Chengdu, China). The escape latency (s) and path length (cm) were analyzed in each trial and averaged over five trials for each rat. The velocity of each rat was also calculated (Mutlu et al. 2015; Zhong et al. 2017).

Histopathological examination

The rats were sacrificed under deep anesthesia by ether inhalation followed by blood-letting, and gross samples of the brain, lung, and heart were taken pictures for pathological injury scoring. Then, specimens of the heart and lung tissue of rats were fixed in 4% paraformaldehyde then embedded in paraffin and serially sectioned and stained with hematoxylin and eosin according to the conventional staining methods (Yu et al. 2014).

Worm collection

Worms were harvested from the lung and brain after sacrificing the rat and were counted under the anatomical microscope. For worms collected from the lung, the average length was calculated by measuring the length of 10 randomly chosen worms from either sex or mixed population. For worms isolated from the brain, 10 worms were randomly chosen from the population for length measurement.

Statistical analysis

The statistical analyses were performed with GraphPad Prism 5.0 (GraphPad Software, Inc., USA) using a one-way analysis of variance (ANOVA) followed by the Tukey-Kramer test. The data were presented as the means ± standard derivation (SD). Differences among the comparisons were considered statistically significant when the P value was less than 0.05. At least three rats were used for Morris water maze neurological function scoring and H&E staining observation.

Results

Rats survival status worsen as *A. cantonensis* infection number increased

To explore the tolerance of rat under different amounts of *A. cantonensis* infection, we monitored the survival status of the infected rat for 35 days by taking advantage of the parameters of body weight and survival rate. The weight of rat in all groups increased during the first 20 days post infection. During 20 to 30 days post infection, for groups G0, G5, and G10, the weight of rats kept growing up; for groups G20 and G40, the body weight showed slight decrease; for the rest groups, the weight of rats dropped gradually (Fig. 1a). Then, we compared the change of rats' body weight between day 0 and day 30. Rats infected with lower dose of parasites gained more weight at the end of infection than that in rats infected with higher dose (Fig. 1b). In groups G280 and G320, the average of rats' weights in day 30 were even less than their original weight (Fig. 1b). Comparing with groups of G0, G5, G10, and G20, the change of weight in groups G280 and G320 was significantly different ($P < 0.001$). Similarly, weight of rats in group G240 decreased significantly when compared with that of rats in groups of G5 and G10 ($P < 0.05$). We also analyzed the survival rate of rats in each

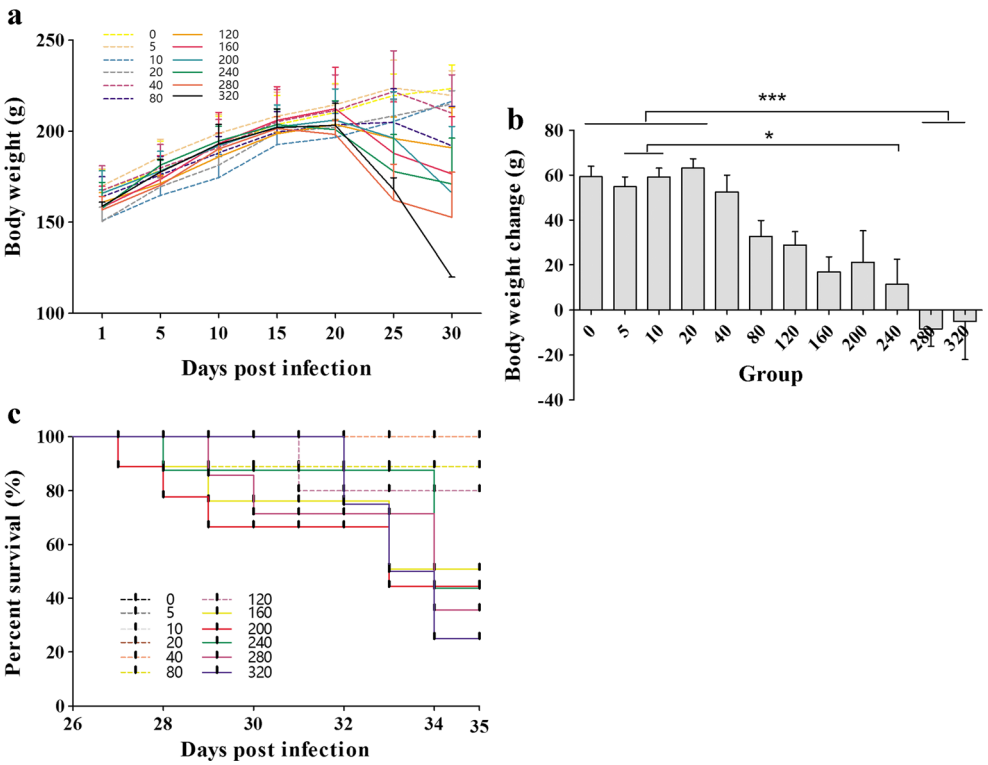

Fig. 1 Survival status of rat in each group after *A. cantonensis* infection. **a** The change of body weight of rat in each group against infection time. **b** The average differences of weight between 30 days post infection and day 0 in each group. The values were presented as the means ± SD of 5 rats per group. *$P < 0.05$, ***$P < 0.001$. **c** The survival rates in each group from day 26 to day 35 post infection. Percent survival = (number of rats alive/5) × 100%

group. From 27-day post-infection, death started to appear in groups with infection number of 80 *A. cantonensis* per rat and above. And the higher the infection rate, the lower the survival rate in the group. Of note, none of the rats died in groups of less than 80 worms per rat (Fig. 1c).

Higher *A. cantonensis* infection dose impaired rat neurological function

In order to understand how the amount of *A. cantonensis* infection affected the rat neurological function, we applied the Morris water maze for evaluation at 21-day post-infection (Fig. 2a). During the first five training trails, no difference in swimming speed was detected among groups (Fig. 2b, c). But we could still observe a decrease trend in the escape latency as the trail increased from the first to the fourth session in all groups (Fig. 2d). The average escape latency of five trails in each group revealed that rats infected with more than 200 worms per rat spent significantly more time than rats infected with 10 and 20 worms per rat ($P < 0.05$) (Fig. 2e), indicating that higher infection amount of *A. cantonensis* impaired rats' spatial learning memory. By analyzing the percentages of time for rats spent swimming to the expected position of the platform, we found that compared with lower infection dose group (infection amount less than 80 *A. cantonensis* per rat) (Fig. 2f1–f5), group with higher infection dose spent more time in the platform quadrant (Fig. 2f6–f12) with a more tanglesome route. What is more, the number that rats passed across the platform was greater in groups with lower infection dose. There is significant difference between uninfected rat group with groups of G160 and G120 ($P < 0.05$ and $P < 0.01$, respectively) (Fig. 2g). In percentage of time spent in the target quadrant, all groups with infection number less than 200 worms per rat had no significant difference in statistics (Fig. 2h).

A. cantonensis infection caused inflammation in multiple organs of the rat

Next, we investigated the damages to rat organs caused by *A. cantonensis* under different infection dose. The brain, lung, and heart were obtained from rat after sacrificing at 35-day post-infection. As the permissive host, at day 35 after infection, the *A. cantonensis* in rat have already migrated from the brain to the lung. As expected, there was no obvious pathological changes in rat brain in groups infected with less than 280 L3 per rat (Fig. 3a–j). In groups G280 and G320, mass bleeding existed underneath the meninges (Fig. 3k, l), demonstrating the higher amount of *A. cantonensis* could also lead to damage in rat brain. By contrast, in the lung of rat, when the infection amount reached 40 worms per rat, evident pulmonary congestion showed up, and the severity increased as the infection dose elevated (Fig. 4a–l). In consistent with the gross observation, after *A. cantonensis* infection, the alveolar spaces were filled with a mixed mononuclear/neutrophilic infiltrate, and the infiltration aggravated as the infection worms increased (Fig. 5a–l), and massive red blood cells infiltrated the alveolar space in groups G280 and G320 (Fig. 5k, l). Similarly, the pathological injury in the heart exacerbated as the infection number of the parasites increased. H&E staining results revealed that no inflammatory response in rat heart when infection dose was lower than 200 worms per rat (Fig. 6a–h). When the number of the infected parasites exceeded 200 per rat, the inflammatory infiltration appeared in serous pericardium and myocardium (Fig. 6i–l). Notably, we also found worm residency in the right atrium and right ventricle of the rats in groups with infection amount above 80 worms per rat (Fig. 6m–o).

The length and sex ratio of recovered *A. cantonensis* changed in rat of high infection number

We harvested *A. cantonensis* from the brain to the lung of the rat in each group at the end of experiment. The overall recovery rate in rat lung showed no significant difference among all groups (Fig. 7a). Then, we counted female and male adult worms from the lung separately, and the female to male ratio increased as the infection number went high (Fig. 7b). Significant differences were observed between the group G20 and the groups infected with above 200 L3 ($P < 0.05$) (Fig. 7b). Besides, the length of worms in each sex were measured. The average length of worms shortened as the infection number increased in both sexes. For female worms, worms in group G320 showed significant shorter length than those in the rest of the groups ($P < 0.001$) (Fig. 7c). The group G280 also owned shorter worm length compared with the groups G40, G80, G120, and G160 ($P < 0.01$) (Fig.7c). Likewise, for male worms, the average length in group G320 was significantly shorter than that in groups G80, G120, and G160 ($P < 0.05$) (Fig. 7d). Taken together, the average length of worms harvested from rat lung decreased in the groups with higher infection number, with significant difference between group G320 and groups G160, G200, and G240 ($P < 0.001$) (Fig. 7e). By contrast, the immature worms collected from the brain had similar body length, significant difference in length was only observed between group G320 and group G200 ($P < 0.05$) (Fig. 7f).

Discussion

Parasitism is one of the most pervasive phenomena in the biological world (Huntley and De Baets 2015). To survive and replicate in the hosts and to complete their life cycles, parasites have evolved elegant strategies (Swann et al. 2015), one of which is to parasitize a wide variety of hosts.

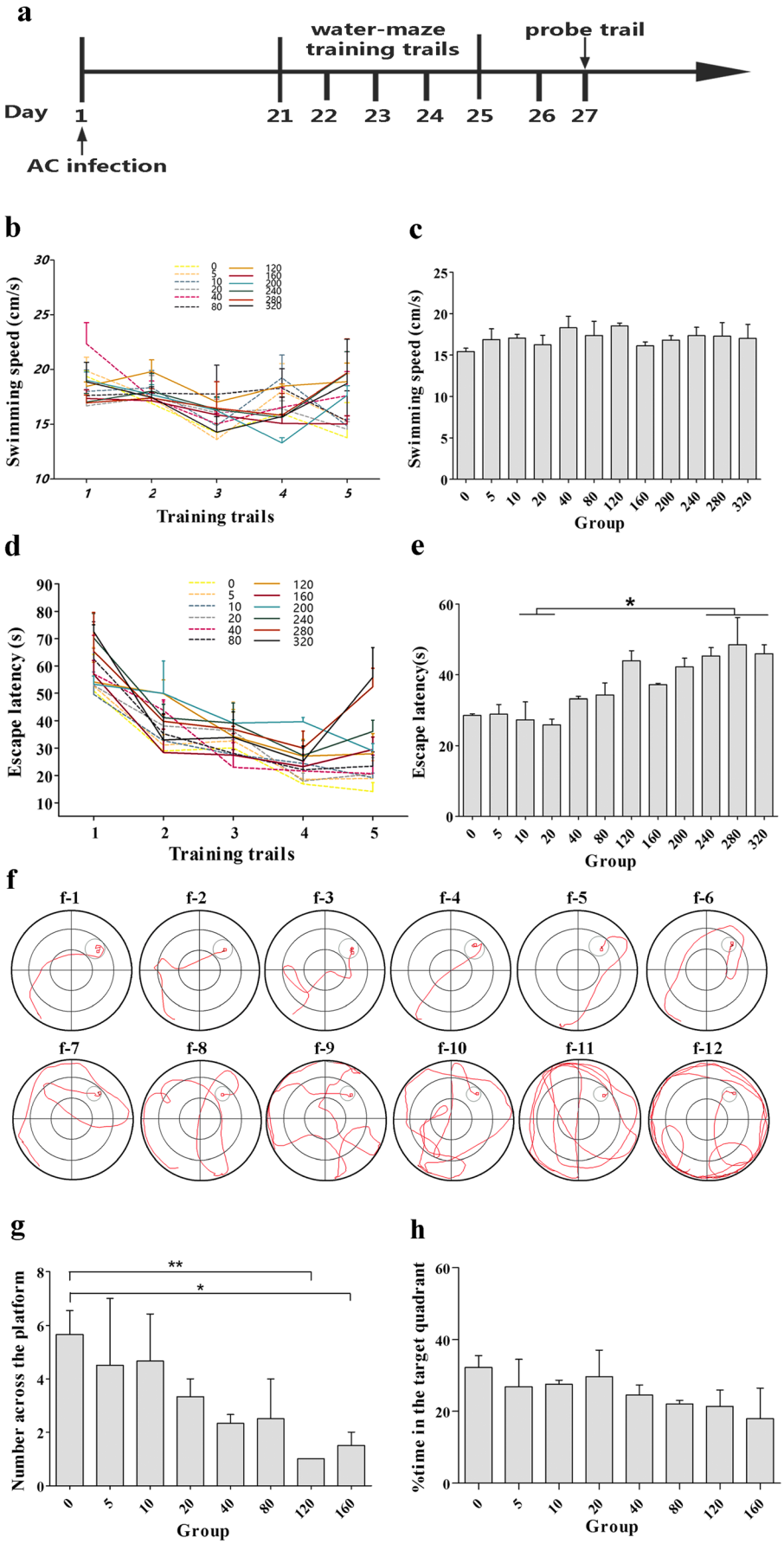

Fig. 2 Effects of *A. cantonensis* infection on rats' spatial learning memory. **a** The schematic of the Morris water maze test for rats. AC meant *A. cantonensis*. The average of swimming speed (**b**) and escape latency (**d**) of each infection group in five training trails. The data were presented as the means ± SD of 5 rats per group. The average of swimming speed (**c**) and escape latency (**e**) in five training trails for each infection group, $*P < 0.05$. The data were means ± SD of 5 rats per group. **f** Representative swim traces of each group in the probe trail. f1 to f12 represented groups with infection rate from 0 to 320 separately. **g** The number for rats across the platform in the trail. Data were presented as the means ± SD. $*P < 0.05$, $**P < 0.01$. **h** Percent of time rats spent in the target quadrant in the task. The values were presented as the means ± SD

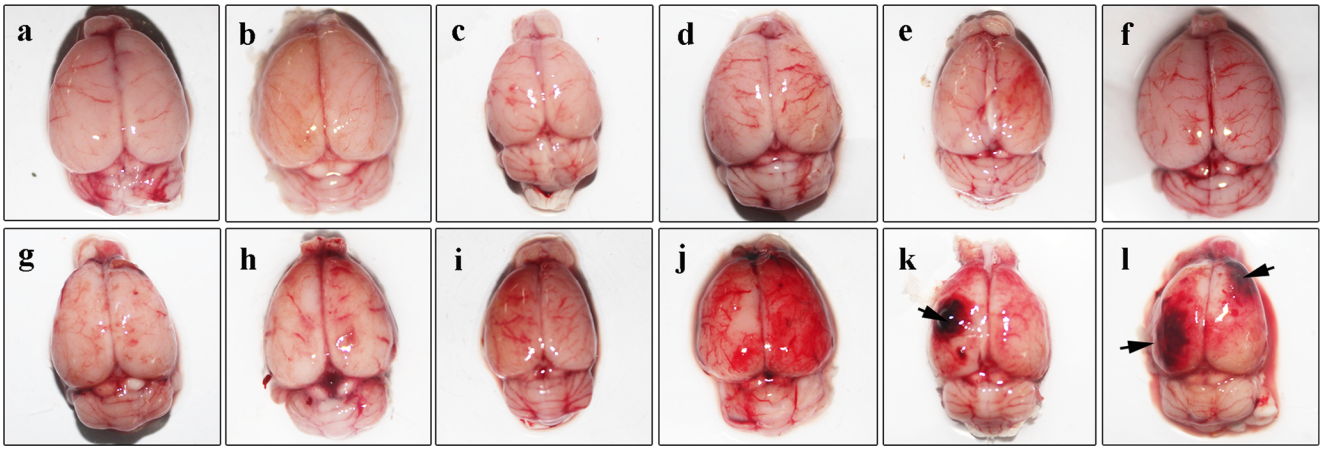

Fig. 3 Representative gross histopathologic photos of rat brain after *A. cantonensis* infection. **a** to **l** represented groups with infection rate from 0 to 320 worms per rat. *Arrows* pointed to the bleeding under meninges

For example, a dozen of mammals can serve as definitive hosts of *Schistosoma japonicum* (Gryseels et al. 2006) and *Clonorchis sinensis* (Liu et al. 2017; Tang et al. 2016), and *Toxoplasma gondii* can invade and survive in all nucleated cells of any warm-blooded animal (Szabo and Finney 2017). Unlike the parasites mentioned above, only a small number of vertebrates, such as rats and hamsters, have been reported as the permissive hosts of *A. cantonensis* hitherto (Wang et al. 2015; Ishii et al. 1980), while mice, monkeys, and human serve as *A. cantonensis* non-permissive hosts, in which the invaded L3 cannot develop into adult worms and failed to maintain the continuity of the life cycle (Qvarnstrom et al. 2016; Wei et al. 2015; Ko 1978). It indicates that *A. cantonensis* and the permissive hosts (rat and hamster) are adapted to each other in the process of coevolution (Papkou et al. 2016). Although rats and mice are both hosts of *A. cantonensis*, the pathological injury to central nerve system caused by the same pathogen, *A. cantonensis*, are distinct in these two animals. As a permissive host, what is the maximum infection number of *A. cantonensis* for rats without leading to death and whether the worm development and recovery rate, sex ratio will be affected by the infection amount in rats are yet unknown.

Our results confirmed that from day 27 after infection, when partial of the fifth stage of larvae (L5) of *A. cantonensis* had migrated from the brain to the lung, rat in groups G80 and above began to die. While in mice model, the death appeared at day 18 when the fourth stage larvae (L4) and L5 resided in the brains of mice. The first death in rat after infection has postponed 9 days compared with that in infected mouse, which is in coincidence with the previous report on the different pathological injury caused by *A. cantonensis* in the permissive host and the non-permissive host (Li et al. 2014a, b; Wang et al. 2015). Meanwhile, it also suggested that unlike mice which were died from severe damage of neural inflammation caused by *A. cantonensis*, the death of rats were attributed to the severe injury on the heart and the lung besides the brain (Figs. 3–6). In addition, none of the rats died in the

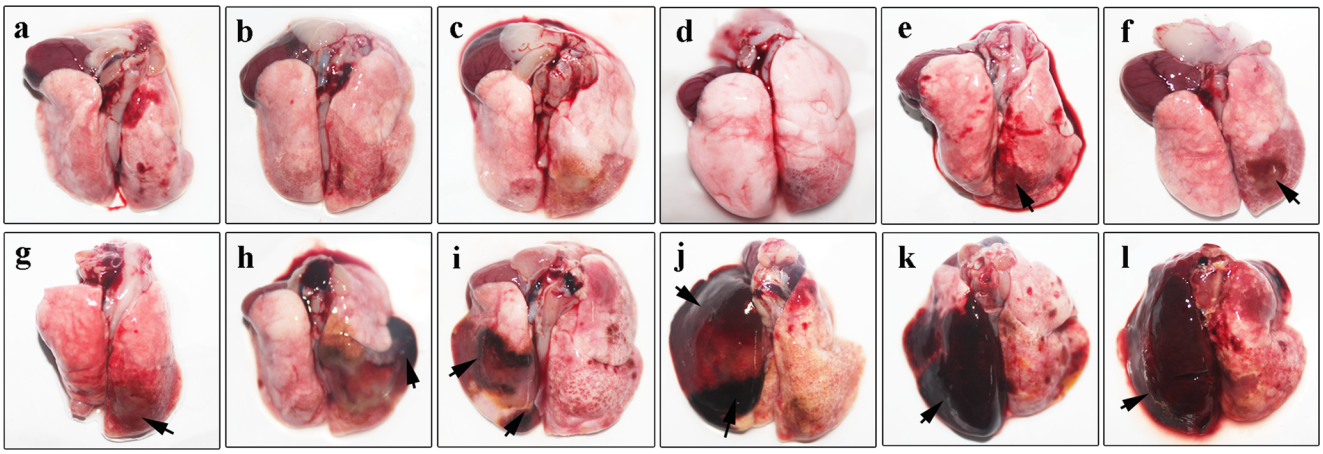

Fig. 4 Representative gross histopathologic pictures of rat lung after *A. cantonensis* infection. Infection rate increased from **a** 0 to **l** 320 worms per rat. *Arrows*: regions showing lung congestion

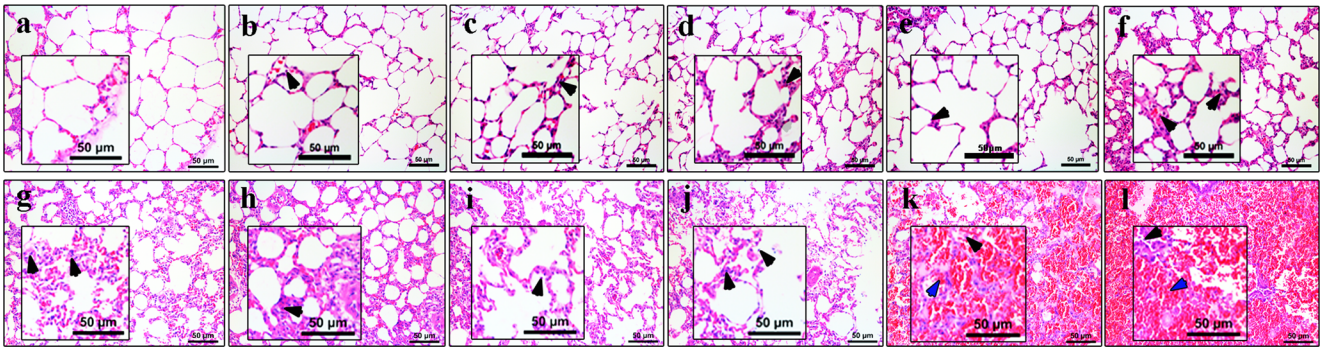

Fig. 5 Representative photomicrographs from lung of rat infected with *A. cantonensis* in each group stained with H&E. **a** to **l** were groups with infection rate ranging from 0 to 320 worms per rat. *Black arrows*: mixed mononuclear/neutrophilic infiltration in the alveolar spaces. *Blue arrows*: massive red blood cell infiltration

groups G5, G10, G20, and G40 at day 35, implying the most appropriate infection dose is 40 *A. cantonensis* per rat for its life cycle maintenance under laboratory conditions.

In the present study, we observed that at day 35 after infection, *A. cantonensis* could migrate and reside into rats' lung which leads to evident swelling and bleeding combining with a large number of eosinophils infiltration (Fig. 5) as the infection dose increased. This observation is consistent with results reported by other researchers (Lan and Lai 2008; Lee et al. 1996). Surprisingly, we also found worm residency in the right atrium and right ventricle of the rats in group G120, leading to severe myocardial inflammation (Fig. 6).

On the other hand, in the parasitic relationship, the host will also have an impact on the parasite. Our results showed that *A. cantonensis* infection dose affected the length and sex ratio of worms collected in rats. Although the recovery rate did not change significantly among groups with different infection amount, the length of worms, either female or male, in groups

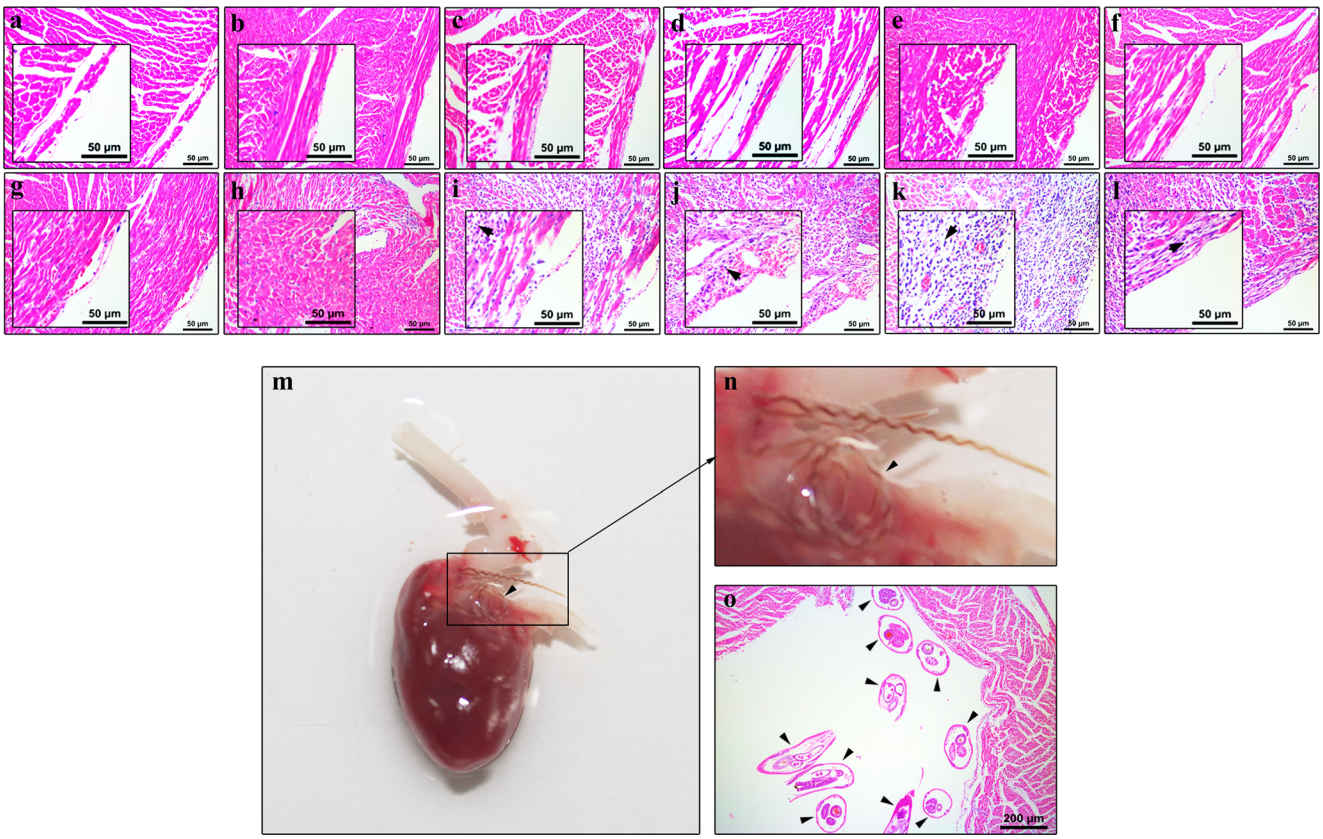

Fig. 6 Representative H&E staining in the heart of rat infected with *A. cantonensis* in each group. From **a** to **l**, the number of *A. cantonensis* for infection went from 0 to 320 worms per rat. *Black arrows*: pericardium and myocardium infiltrated with a mixed mononuclear/neutrophilic. **m**–**o** *A. cantonensis* were found residency in the rat right atrium and right ventricle. *Black arrow*: *A. cantonensis* worm in the gross heart sample. **n** Enlarged photo of the rectangle region in (**m**). **o** H&E staining of the region (**n**). *Arrows*: *A. cantonensis* worm

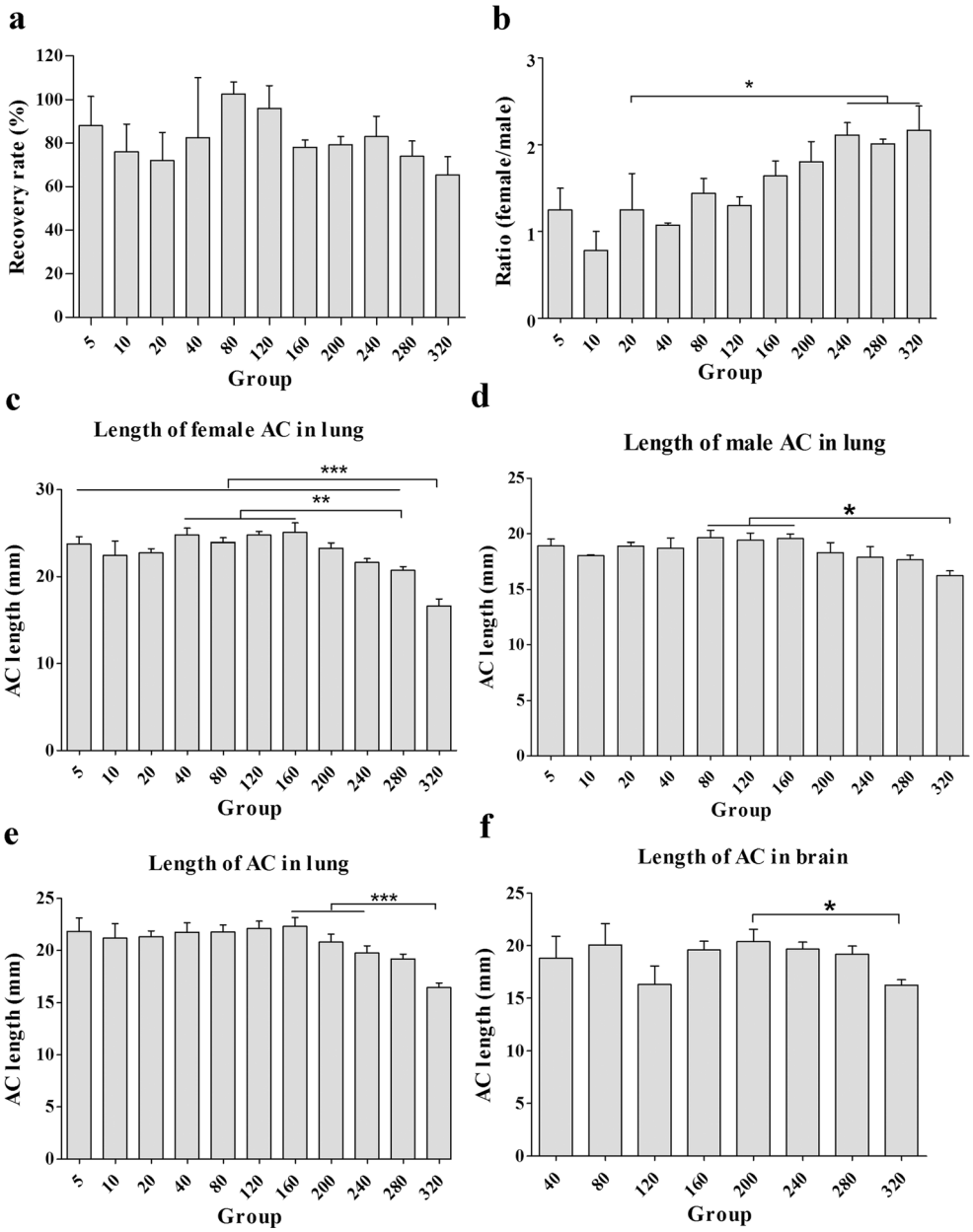

Fig. 7 The length and sex ratio of *A. cantonensis* collected from infected rats. **a** Recovery rate of *A. cantonensis* harvested from lung of infected rat. Recovery rate = (number of worm collected/number of worm infected) × 100%. **b** Female to male ratio of worms harvested from rat lung. **c** The length of female (**c**), male (**d**), and worms of both sex (**e**) collected in infected rat lung. **f** Length of worms collected in the brain of infected rat. All data represented were means ± SD. $^{*}P < 0.05$, $^{**}P < 0.01$, $^{***}P < 0.001$

with higher infection dose (280 or 320 *A. cantonensis* per rat) were significantly shorter than that in groups with lower infection dose (160 L3 per animal). It is probably due to the intense competition for nutrition and living space and higher environmental pressure under high parasite density (Paterson and Viney 2002; Reynolds et al. 2016; Hirao and Ehlers 2008). Interestingly, we also noticed that the ratio of female to male worm increased as the infection dose elevated, which could be the consequence of higher selective pressure in the dense nematodes population (Therese and Bashey 2012; Haukisalmi et al. 1996).

In summary, our results demonstrated that although rat has been considered as a permissive host for *A. cantonensis*, overdose (more than 80 *A. cantonensis* per rat) infection can lead to their death, which could be ascribed to the inflammatory injury in multiple organs for instance, the brain, heart, and lung. Besides, the length of the worms collected in rats' lung and the ratio between female and male worms were inversely correlated with the infection dose. Hence, our findings have enriched the understanding of the interaction between *A. cantonensis* and its host as well as the adaptability and tolerance between them.

Acknowledgements This work was supported by grants from the National Key Research and Development Program of China (grant no. 2016YFC1202003, 2016YFC1202005, and 2016YFC1200500), the National Natural Science Foundation of China (grant no. 81371836, 81572023, 81271855, 81261160324, and 81401689), Project of Basic Platform of National Science and Technology Resources of the

Ministry of Sciences and Technology of China (grant no. TDRC-2017-22), Guangdong Natural Science Foundation (grant no. 2014A030313134 and 2014A030310228), Science and Technology Planning Project of Guangdong Province (grant no. 2016A050502008), Science and Technology Planning Project of Guangzhou (grant no. 201607010029), the Undergraduates Innovation Training Program of Guangdong Province (201410558274, 201601084), and the Laboratory of Parasite and Vector Biology, MOPH (grant no. WSBKTKT201401).

References

Chen HT (1935) Un nouveau nematode pulmonaire, Pulmonem *A. cantonensis* n.g., n. sp. des rats de Canton. Ann Parasitol 13(4): 312–317

Eamsobhana P (2014) Eosinophilic meningitis caused by *Angiostrongylus cantonensis*—a neglected disease with escalating importance. Trop Biomed 31(4):569–578

Feng F, Feng Y, Liu Z, Li WH, Wang WC, Wu ZD, Lv Z (2015) Effects of albendazole combined with TSII-A (a Chinese herb compound) on optic neuritis caused by *Angiostrongylus cantonensis* in BALB/c mice. Parasit Vectors 25(8):606

Gryseels B, Polman K, Clerinx J, Kestens L (2006) Human schistosomiasis. Lancet 368(9541):1106–1118

Haukisalmi V, Henttonen H, Vikman P (1996) Variability of sex ratio, mating probability and egg production in an intestinal nematode in its fluctuating host population. Int J Parasitol 26(7):755–763

Hirao A, Ehlers RU (2008) Influence of nematode inoculum density and temperature on development of *Steinernema carpocapsae* and *S. feltiae* in liquid culture. Commun Agric Appl Biol Sci 73(4): 699–702

Huntley JW, De Baets K (2015) Trace fossil evidence of trematode-bivalve parasite-host interactions in deep time. Adv Parasitol 90: 201–231

Ishii AI, Kino H, Hayashi M, Fujio Y, Sano M (1980) Experimental light infection of *Angiostrongylus cantonensis* in hamsters. Int J Zoonoses 7(2):120–124

Jiang J, Gao K, Zhou Y, Xu A, Shi S, Liu G, Li Z (2015) Electroacupuncture treatment improves learning-memory ability and brain glucose metabolism in a mouse model of Alzheimer's disease: using Morris water maze and Micro-PET. Evid Based Complement Alternat Med 2015:142129

Ko RC (1978) Occurrence of *Angiostrongylus cantonensis* in the heart of a spider monkey. J Helminthol 52(3):229

Lan KP, Lai SC (2008) *Angiostrongylus cantonensis*: induction of urokinase-type PA and degradation of type IV collagen in rat lung granulomatous fibrosis. Exp Parasitol 118(4):472–477

Lee HH, Jiang ST, Shyu LY, Lin WL, Chian HC, Hsu CC, Chou FP, Wang CJ (1996) L ferritin accumulation in macrophages infiltrating the lung during rat *Angiostrongylus cantonensis* infection. Exp Parasitol 83(1):55–61

Li S, Yang F, Ji P, Zeng X, Wu X, Wei J, Ouyang L, Liang J, Zheng H, Wu Z, Lv Z (2014a) Eosinophil chemotactic chemokine profilings of the brain from permissive and non-permissive hosts infected with *Angiostrongylus cantonenis*. Parasitol Res 113(2):517–525

Li Z, Chen X, Zen X, Liang J, Wei J, Lv Z, Sun X, Wu ZD (2014b) MicroRNA expression profile in the third- and fourth-stage larvae of *Angiostrongylus cantonensis*. Parasitol Res 113(5):1883–1896

Liu Z, Wu Y, Feng Y, Wu F, Liu RF, Wang LF, Liang JY, Liu JH, Sun X, Wu ZD (2017) Spleen atrophy related immune system changes attributed to infection of *Angiostrongylus cantonensis* in mouse model. Parasitol Res 116(2):577–587

Lv S, Zhang Y, Liu HX, Hu L, Yang K, Steinmann P, Chen Z, Wang LY, Utzinger J, Zhou XN (2009) Invasive snails and an emerging infectious disease: results from the first national survey on *Angiostrongylus cantonensis* in China. PLoS Negl Trop Dis 3(2):e368

McBride A, Chau TT, Hong NT, Mai NT, Anh NT, Thanh TT, Van TT, Xuan LT, Sieu TP, Thai LH, Chuong LV, Sinh DX, Phong ND, Phu NH, Day J, Nghia HD, Hien TT, Chau NV, Thwaites G, Tan LV (2017) *Angiostrongylus cantonensis* is an important cause of eosinophilic meningitis in southern Vietnam. Clin Infect Dis. doi:10.1093/cid/cix118

Mutlu O, Akar F, Celikyurt IK, Tanyeri P, Ulak G, Erden F (2015) 7-NI and ODQ disturbs memory in the elevated plus maze, Morris water maze, and radial arm maze tests in mice. Drug Target Insights 9:1–8

New D, Little MD, Cross J (1995) *Angiostrongylus cantonensis* infection from eating raw snails. N Engl J Med 332(16):1105–1106

Papkou A, Gokhale CS, Traulsen A, Schulenburg H (2016) Host-parasite coevolution: why changing population size matters. Zoology (Jena) 119(4):330–338

Paterson S, Viney ME (2002) Host immune responses are necessary for density dependence in nematode infections. Parasitology 125(Pt 3): 283–292

Qvarnstrom Y, Xayavong M, da Silva AC, Park SY, Whelen AC, Calimlim PS, Sciulli RH, Honda SA, Higa K, Kitsutani P, Chea N, Heng S, Johnson S, Graeff-Teixeira C, Fox LM, da Silva AJ (2016) Real-time polymerase chain reaction detection of *Angiostrongylus cantonensis* DNA in cerebrospinal fluid from patients with eosinophilic meningitis. AmJTrop Med Hyg 94(1):176–181

Reynolds A, Lindström J, Johnson PC, Mable BK (2016) Evolution of drug-tolerant nematode populations in response to density reduction. Evol Appl 9(5):726–738

Swann J, Jamshidi N, Lewis NE, Winzeler EA (2015) Systems analysis of host-parasite interactions. Wiley Interdiscip Rev Syst Biol Med 7(6): 381–400

Szabo EK, Finney CA (2017) *Toxoplasma gondii*: one organism, multiple models. Trends Parasitol 33(2):113–127

Tang ZL, Huang Y, Yu XB (2016) Current status and perspectives of *Clonorchis sinensis* and clonorchiasis: epidemiology, pathogenesis, omics, prevention and control. Infect Dis Poverty 5(1):71

Therese MO, Bashey F (2012) Natal-host environmental effects on juvenile size, transmission success, and operational sex ratio in the entomopathogenic nematode *Steinernema carpocapsae*. J Parasitol 98(6):1095–1100

Tsai HC, Lee SS, Huang CK, Yen CM, Chen ER, Liu YC (2004) Outbreak of eosinophilic meningitis associated with drinking raw vegetable juice in southern Taiwan. AmJTrop Med Hyg 71(2):222–226

Wang QP, Wu ZD, Wei J, Owen RL, Lun ZR (2012) Human *Angiostrongylus cantonensis*: an update. Eur J Clin Microbiol Infect Dis 31(4):389–395

Wang LC, Jung SM, Chen KY, Wang TY, Li CH (2015) Temporal-spatial pathological changes in the brains of permissive and non-permissive hosts experimentally infected with *Angiostrongylus cantonensis*. Exp Parasitol 157:177–184

Wei J, Wu F, He A, Zeng X, Ouyang LS, Liu MS, Zheng HQ, Lei WL, Wu ZD, Lv ZY (2015) Microglia activation: one of the checkpoints in the CNS inflammation caused by *Angiostrongylus cantonensis* infection in rodent model. Parasitol Res 114(9):3247–3254

Yu L, Liao Q, Zeng X, Lv Z, Zheng H, Zhao Y, Sun X, Wu Z (2014) MicroRNA expressions associated with eosinophilic meningitis caused by *Angiostrongylus cantonensis* infection in a mouse model. Eur J Clin Microbiol Infect Dis 33(8):1457–1465

Zhang L, Fang Y, Lian Y, Chen Y, Wu T, Zheng Y, Zong H, Sun L, Zhang R, Wang Z, Xu Y (2015) Brain-derived neurotrophic factor ameliorates learning deficits in a rat model of Alzheimer's disease induced by aβ1-42. PLoS One 10(4):e0122415

Zhong W, Yang M, Zhang W, Visocchi M, Chen X, Liao C (2017) Improved neural microcirculation and regeneration after peripheral nerve decompression in DPN rats. Neurol Res 14:1–7